Supporting Information

Mobility Evaluation of BTBT Derivatives: Limitation and Impact on Charge Transport

Robert Wawrzinek,[a,b,†] Jan Sobus,[a,b,†] Mujeeb Ullah Chaudhry,[a,b] Viqar Ahmad,[a,b] Arnaud Grosjean,[c] Jack K. Clegg,[c] Ebinazar B. Namdas[a,b,*] and Shih-Chun Lo[a,c,*]

[a] Centre for Organic Photonics & Electronics, The University of Queensland, Brisbane, Queensland 4072, Australia
[b] School of Mathematics and Physics, The University of Queensland, Brisbane, Queensland 4072, Australia.
[c] School of Chemistry and Molecular Biosciences, The University of Queensland, Brisbane, Queensland 4072, Australia.

[*]Correspondence to: s.lo@uq.edu.au and e.namdas@uq.edu.au;

[†] RW and JS contributed equally.

Table S1. Reported mobilities of alkylated BTBT derivatives (selection).

Material	μ_h [cm^2/Vs]	Deposition	Substrate	Comments	Reference
BTBT	–	vacuum		no values due to poor film quality	1
BTBT-C_8					
BTBT-C_{10}	5	vacuum	SiOx		2
C_8-BTBT-C_8	3.5–6	solution	SiO_2/Si	treated with (F4-TCNQ) solution	3
	3.5–7.4	solution	SiO_2/Si	solvent vapour annealed	4
	4–6	solution	SiO_2/Si	directional solidification via temperature gradients	5
	4	solution	Si		6
	16.4	solution	SiO_2/Si	Ink-jet printed	7
	10	vacuum	Graphene; BN	monolayer crystals	8
	4.8	solution	SiO_2/Si	floating-coffee-ring-driven assembly	9
	0.5–1.8	solution	SiO_2/Si	study also on C_x-BTBT-C_x (x = 5–14)	10
	25	solution	Si/ITO	off-centre spin coating	11
	0.3–2.9	solution	SiO_2; OTS; ODTS		12
	3.0	solution	SiO_2/Si + PMMA	solvent vapour annealed	13
	0.53	solution	Phenyl-SAM on flexible substrate	surface-selective deposition technique	14
	1.2	solution	SiO_2/Si	off-centre re spin coating	15
	30	chemical vapour		graphene monolayer on C_8-BTBT-C_8 bilayer	16
	1.0	vacuum	PMMA		17
	1.82	vacuum	pC_1D_1		18
	1.4–3.9	vacuum	SiO_2/Si	discussion mobility calculation by van der Pauw method	19
	1.4	vacuum	SiO_2/Si	cross-linkable high-*k* polymer matrix	20
	7.9	solution	SiO_2/Si		21
	1.68	solution	SiO_2/Si	dip-coating deposition	22

	1.42	solution	a-alumina/KPI		23
	16	solution	SiO_2/Si	mobility up to 52 cm^2/Vs at 80 K	24
	1.2	solution/OMBD	SiO_2/Si	organic molecular beam deposition (OMBD)	15
	7.22	solution	OTS-Si & C-PVA	380 nm thin films	25
	12	solution	SiO_2/Si	BTBT-C_8-polystyrene blends	26
C_{10}-BTBT-C_{10}	0.5–1.8	solution	SiO_2/Si	study also on C_x-BTBT-C_x (x = 5–14)	10
	0.4–2.7	solution	SiO_2; OTS; ODTS		12
	0.2–0.56	solution		surface modified polyimide gate insulator	27
BTBT-C_{12}	0.53–3.9	solution	SiO_2; OTS; ODTS		12
	(170)*	solution	SiO_2; PMMA	*mobilitiy determined *via* FI-TRMC	28
BTBT-C_{13}	14.2	vacuum	AlOx+SAMs	SAMs = alkyl phosphonic acids	29
	5.7	vacuum	AlOx+ SAMs+Salts	SAMs = oligo-ethylene-glycol phosphonic acid; Salts = LiCl, NaCl, KCl	30
Ph-BTBT-C_{10}	4.9	solution	SiO_2/Si^+ polystyrene	thermally annealed	31
	12	solution	SiO_2/Si	thermally annealed	32
	48	solution	SiO_2/Si	Single crystal	33
Ph-BTBT-C_{12}	8.7	vacuum	SiO_2/Si	thermally annealed	34

General Methods

All commercial reagents and chemicals were used as received unless otherwise noted. Petroleum with boiling point range 40–60 °C was distilled before use. Solvent ratio used for column chromatography is reported by volume. All ^{1}H NMR spectra were recorded on Bruker Avance 300 spectrometer in deuterated $CHCl_3$, which was neutralised by passing through a glass pipette of aluminium oxide, with chemical shifts (δ) reported in parts per million (ppm) and are referenced to the residual solvent peak, *i.e.*, δ 7.26 ppm for ^{1}H NMR. Multiplicities are reported as singlet (s), doublet (d), triplet (t), and multiplet (m); Ar-H = aromatic H. All coupling constants (*J*) are in Hertz (Hz) and rounded to the nearest 0.5 Hz. Melting points (m.p.) were measured in a glass capillary on a BÜCHI Melting Point B-545 and are uncorrected. Thermal gravimetric analysis (TGA) measurements were carried out on a Perkin Elmer STA 6000 under 10 °C/min of nitrogen flow and the TGA temperature was quoted at 5% weight loss. Infrared spectra were recorded on a Perkin Elmer Spectrum 1000 FT-IR spectrometer as solid state samples. High resolution electrospray ionisation (HRESIMS) accurate mass measurements were carried out on a Bruker MicrOTOF-Q (quadrupole – Time of Flight) instrument with a Bruker ESI source at the School of Chemistry & Molecular Biosciences, the University of Queensland, by Mr Graham MacFarlane. Accurate mass measurements are carried out with external calibration (using Agilent tune mix as the reference calibrant) followed by a one point linear correction internal calibration using the diisooctyl phthalate $[M+Na]^+$ m/z 413 peak in positive ion. Elemental microanalyses were carried out at the School of Chemistry & Molecular Biosciences, the University of Queensland, on a FLASH 2000 CHNS/O Analyzer by Mr Michael Nefedov, MD. PhD. Absorption spectra were recorded on a Varian Cary 5000 UV-Vis-NIR spectrophotometer in 10 x 10 mm quartz cuvettes or on quartz substrates. Fluorescence spectra were measured using a Jobin-Yvon Horiba Fluorolog in steady-state mode using a xenon lamp as the excitation source.

Synthesis

BTBT,[35] **BTBT-C$_8$**,[36,37] **BTBT-C$_{10}$**,[38] **C$_8$-BTBT-C$_8$**[10] and **C$_{10}$-BTBT-C$_{10}$**[10] were synthesised by following literature procedures. Scheme S1 shows the synthetic route used.

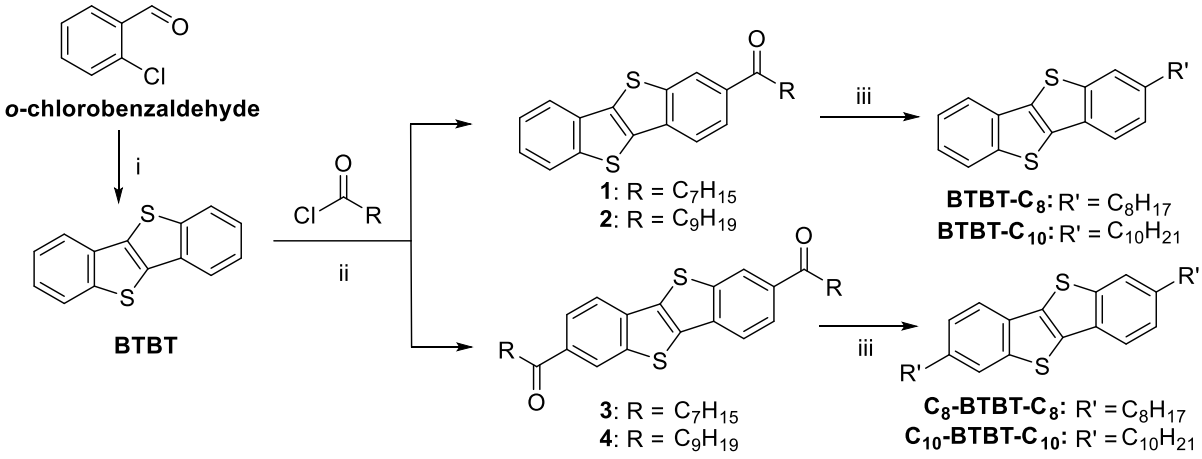

Scheme S1. Synthetic route to alkylated BTBT derivatives: i) sodium hydrosulfide hydrate, 1-methyl-2-pyrrolidinone; ii) $AlCl_3$, CH_2Cl_2, acyl chloride; iii) KOH, diethylene glycol, hydrazine hydrate.

[1]Benzothieno[3,2-*b*][1]benzothiophene, BTBT

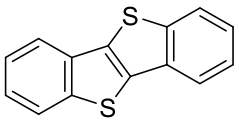

Sodium hydrosulfide hydrate (70%, 22.8 g, 285 mmol) was added to a solution of *o*-chlorobenzaldehyde (16 mL, 142 mmol) in 31 mL anhydrous 1-methyl-2-pyrrolidinone at 80 °C under argon. The reaction mixture was stirred for 1 h and subsequently heated to 200 °C and stirred for 12 h at this temperature. The mixture was allowed to cool to room temperature and 150 mL ice water were added. The resulting precipitate was filtered, washed with water (50 mL) and recrystallised from toluene to give **BTBT** (4.20 g, 25%) as white crystals; m.p. 214 °C; ^{1}H NMR (300 MHz, $CDCl_3$): δ 7.36−7.53 (4H, m, Ar-H), 7.85−7.97 (4H, m, Ar-H).

1-(Benzo[*b*]benzo[4,5]thieno[2,3-*d*]thiophen-2-yl)octan-1-one, 1

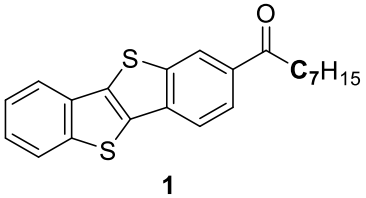

BTBT (1.50 g, 6.24 mmol) was stirred in 150 mL dry dichloromethane and cooled to -20 °C under argon. $AlCl_3$ (3.00 g, 22.5 mmol) was added in one portion and the reaction mixture was cooled down -78 °C. *n*-Octanoyl chloride (4.26 mL, 25.0 mmol) were added dropwise (over 20 min) to the mixture and the reaction was allowed to warm up to room temperature over 12 h. After quenching with 120 mL ice water dichloromethane

(~100 mL) was added to dissolve the resultant precipitate. The organic layer was separated and the solvent removed under vacuum. The residue was purified by recrystallization from toluene and subsequently column chromatography over silica using toluene/petroleum (1:3) as eluent to give **1** (1.10 g, 48%) as a white solid; m.p. 178−180 °C (lit.:[37] 177−180 ºC); ^{1}H NMR (300 MHz, $CDCl_3$): δ 0.90 (3H, t, *J* = 7.0 Hz, CH_3), 1.24−1.48 (8H, m, CH_2), 1.74−1.87 (2H, m, CH_2), 3.07 (2H, t, *J* = 7.5 Hz, CH_2), 7.43−7.54 (2H, m, Ar-H), 7.90−7.97 (3H, m, Ar-H), 8.06 (1H, dd, *J* = 8.5, 1.5 Hz, Ar-H), 8.55 (1H, dd, *J* = 1.5, 0.5 Hz, Ar-H).

1-(Benzo[*b*]benzo[4,5]thieno[2,3-*d*]thiophen-2-yl)decan-1-one, 2

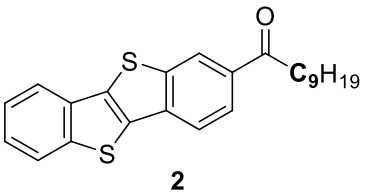

2

BTBT (1.50 g, 6.24 mmol) was stirred in 150 mL dry dichloromethane and cooled to -20 °C under argon. $AlCl_3$ (3.00 g, 22.5 mmol) was added in one portion and the reaction mixture was cooled down -78 °C. *n*-Decanoyl chloride (5.18 mL, 25.0 mmol) was added dropwise over 20 min and thee reaction mixture was allowed to warm up to room temperature over 12h. After quenching with 50 mL ice water. The organic layer was separated and the solvent reduced down to 50 mL under vacuum. Methanol (50 mL) was added and the resulting precipitate filtered. The aqueous layer was filtered as well and both filtrates were washed with water (3 x 50 mL) and methanol (3 x 50 mL). Filtrates were purified by recrystallization from a toluene/petroleum mixture (1:10) to give **2** (1.80 g, 73%) as a white solid; m.p. 172 °C; ^{1}H NMR (300 MHz, $CDCl_3$): δ 0.88 (3H, t, *J* = 7.0 Hz, CH_3), 1.21−1.48 (12H, m, CH_2), 1.73−1.87 (2H, m, CH_2), 3.07 (2H, t, *J* = 6.0 Hz, CH_2), 7.42−7.53 (2H, m, Ar-H), 7.90−7.98 (3H, m, Ar-H), 8.06 (1H, dd, *J* = 8.5, 1.5 Hz, Ar-H), 8.54−8.57 (1H, m, Ar-H).

1,1'-(Benzo[*b*]benzo[4,5]thieno[2,3-*d*]thiophene-2,7-diyl)bis(octan-1-one), 3

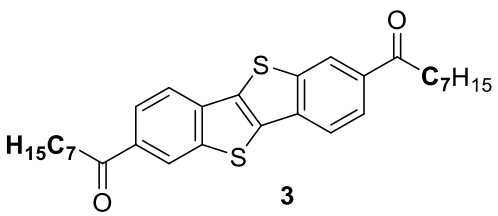

3

BTBT (1.00 g, 4.16 mmol) was stirred in 100 mL dry dichloromethane and cooled to -20 °C under argon. $AlCl_3$ (3.05 g, 22.9 mmol) was added in one portion and the reaction mixture was cooled down -78 °C. *n*-Octanoyl chloride (3.55 mL, 20.8 mmol) was added dropwise over 20 min and the reaction mixture was allowed to warm up to room temperature over 12 h. After quenching with 50 mL ice water the resulting precipitate was filtered and consequently washed with water (3 x 50 mL) and MeOH (3 x 50 mL). The precipitate was purified by recrystallization from toluene to give **3** (1.18 g, 58%) as a white solid; m.p. 252 °C (lit.:[10] 250−251 ºC); ^{1}H NMR (300 MHz, $CDCl_3$): δ 0.9 (6H, t, *J* = 7.0 Hz, CH_3), 1.24−1.49

(16H, m, CH_2), 1.73−1.87 (4H, m, CH_2), 3.08 (4H, t, *J* = 7.0 Hz, CH_2), 7.98 (2H, dd, *J* = 8.5, 0.5 Hz, Ar-H), 8.08 (2H, dd, *J* = 8.5, 1.5 Hz, Ar-H), 8.57 (2H, dd, *J* = 1.5, 0.5 Hz, Ar-H).

1,1'-(Benzo[*b*]benzo[4,5]thieno[2,3-*d*]thiophene-2,7-diyl)bis(decan-1-one), 4

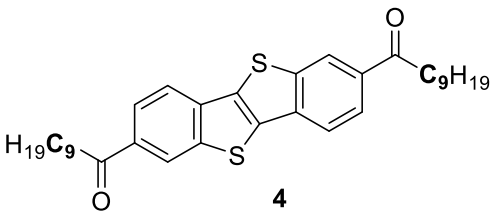

4

BTBT (1.00 g, 4.16 mmol) was stirred in 100 mL dry dichloromethane and cooled to -20 °C under argon. $AlCl_3$ (3.05 g, 22.9 mmol) was added in one portion and the reaction mixture was cooled down -78 °C. *n*-Decanoyl chloride (4.32 mL, 20.8 mmol) was added dropwise over 20 min. The reaction mixture was allowed to warm up to room temperature and stirred at room temperature for 2 days. After quenching with 50 mL ice water the resulting precipitate was filtered and washed with water (3 x 50 mL) and MeOH (3 x 50 mL). The precipitate was purified by recrystallization from toluene to give **4** (825 mg, 36%) as a white solid; m.p. 246 °C (lit.:[10] 241−242 °C); ^{1}H NMR (300 MHz, $CDCl_3$): δ 0.89 (6H, t, *J* = 7.0 Hz, CH_3), 1.24−1.47 (24H, m, CH_2), 1.74−1.87 (4H, m, CH_2), 3.08 (4H, t, *J* = 7.5 Hz, CH_2), 7.98 (2H, d, *J* = 8.0 Hz, Ar-H), 8.09 (2H, dd, *J* = 8.5, 1.5 Hz, Ar-H), 8.57 (2H, d, *J* = 1.0 Hz, Ar-H).

2-Octylbenzo[*b*]benzo[4,5]thieno[2,3-*d*]thiophene, BTBT-C_8

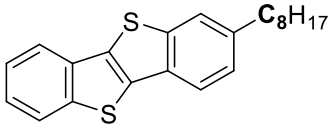

BTBT-C_8

Hydrazine hydrate (55%, 3.4 mL, 38.2 mmol) was added to a suspension of **2** (1.12 g, 3.06 mmol) and freshly pulverised KOH (860 mg, 15.3 mmol) in 44 mL diethylene glycol. The reaction mixture was heated to 200 °C (oil bath temperature) and stirred for 12 h. After the mixture was allowed to cool down to room temperature and poured into 40 mL of methanol, the resulting precipitate was filtered, washed with water (3 x 20 mL) and methanol (3 x 20 mL) and subsequently purified by column chromatography over silica using toluene/petroleum 2:1 as eluent, followed by recrystallization from toluene/petroleum (1:10) to give **BTBT-C_8** (463 mg, 43%) as white crystals ; (m.p. 115 °C; lit.:[37] 113−115 °C); ^{1}H NMR (300 MHz, $CDCl_3$): δ 0.89 (3H, t, *J* = 7.0 Hz, CH_3), 1.23−1.44 (10H, m, CH_2), 1.64−1.77 (2H, m, CH_2), 2.76 (2H, t, *J* = 8.0 Hz, CH_2), 7.29 (1H, dd, *J* = 8.0, 1.5 Hz, Ar-H), 7.35−7.49 (2H, m, Ar-H), 7.72 (1H, dd, *J* = 1.5, 0.5 Hz, Ar-H), 7.79 (1H, d, *J* = 8.0 Hz, Ar-H), 7.84−7.94 (2H, m, Ar-H); IR ν_{max}(solid)/cm^{-1}: 2919, 2849, 1465, 1449, 1427, 1335, 1255, 954, 814, 741, 722; m/z HRMS (ESI-MS): calculated for $C_{22}H_{24}NaS_2$ $[M+Na]^+$: 375.1212; found $[M+Na]^+$: 375.1208; $C_{22}H_{24}S_2$ requires C, 75.0; H, 6.9; S, 18.2%; found: C, 75.0; H, 6.9; S, 18.6%.

2-Decylbenzo[*b*]benzo[4,5]thieno[2,3-*d*]thiophene, BTBT-C$_{10}$

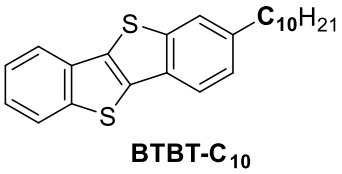

BTBT-C$_{10}$

Hydrazine hydrate (55%, 11 mL, 124 mmol) was added to a suspension of **1** (3.92 g, 9.93 mmol) and freshly pulverised KOH (2.79 mg, 49.7 mmol) in 120 mL diethylene glycol. The reaction mixture was heated to 200 °C (oil bath temperature) and stirred for 24 h. After the mixture was allowed to cool down to room temperature and poured into 150 mL of methanol, the resulting precipitate was filtered, washed with water (3 x 80 mL) and methanol (3 x 80 mL) and subsequently purified by column chromatography over silica using toluene/ petroleum (2:1) as eluent to give **BTBT-C$_{10}$** (3.34 g, 88%) as white crystals; (m.p. 110 °C); ^{1}H NMR (300 MHz, $CDCl_3$): δ 0.88 (3H, t, *J* = 7.0 Hz, CH_3), 1.22−1.43 (14H, m, CH_2), 1.64−1.77 (2H, m, CH_2), 2.76 (2H, t, *J* = 8.0 Hz, CH_2), 7.28 (1H, dd, *J* = 8.0, 1.5 Hz, Ar-H), 7.35−7.50 (2H, m, Ar-H), 7.71−7.74 (1H, m, Ar-H), 7.79 (1H, d, *J* = 8.0 Hz, Ar-H), 7.84−7.94 (2H, m, Ar-H); IR ν_{max}(solid)/cm^{-1}: 2916, 2848, 1464, 1449, 1428, 1335, 1255, 814, 741, 722; m/z HRMS (ESI-MS): calculated for $C_{24}H_{28}NaS_2$ $[M+Na]^+$: 403.1525; found $[M+Na]^+$: 403.1528; $C_{24}H_{28}S_2$ requires C, 75.7; H, 7.4; S, 16.9%; found: C, 75.4; H, 7.4; S, 16.8%.

2,7-Dioctylbenzo[*b*]benzo[4,5]thieno[2,3-*d*]thiophene, C$_8$-BTBT-C$_8$

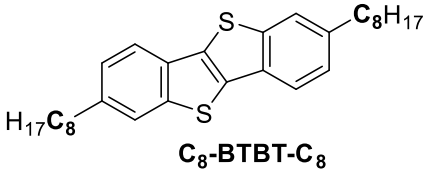

C$_8$-BTBT-C$_8$

Hydrazine hydrate (55%, 4.9 mL, 55.8 mmol) was added to a suspension of **3** (1.10 g, 2.23 mmol) and freshly pulverised KOH (1.25 mg, 22.3 mmol) in 44 mL diethylene glycol. The reaction mixture was heated to 220 °C (oil bath temperature) and stirred for 18 h. After the mixture was allowed to cool down to room temperature and poured into 40 mL of methanol, the resulting precipitate was filtered, washed with water (3 x 20 mL) and methanol (3 x 20 mL) and subsequently purified by column chromatography over silica using petroleum to give **C$_8$-BTBT-C$_8$** (631 mg, 61%) as white crystals; (m.p. 111−112 °C); ^{1}H NMR (300 MHz, $CDCl_3$): δ 0.89 (6H, t, *J* = 7.0 Hz, CH_3), 1.21−1.44 (20H, m, CH_2), 1.63−1.77 (4H, m, CH_2), 2.76 (4H, t, *J* = 8.0 Hz, CH_2), 7.26 (1H, d, *J* = 1.5 Hz, Ar-H), 7.28 (1H, d, *J* = 1.5 Hz, Ar-H), 7.70 (2H, dd, *J* = 1.5, 0.5 Hz, Ar-H), 7.76 (2H, dd, *J* = 8.0, 0.5 Hz, Ar-H); IR ν_{max}(solid)/cm^{-1}: 2918, 2848, 1459, 1336, 951, 879, 814, 792, 719, 610; m/z HRMS (ESI-MS): calculated for $C_{30}H_{40}NaS_2$ $[M+Na]^+$: 487.2464; found $[M+Na]^+$: 487.2458; $C_{30}H_{40}S_2$ requires C, 77.5; H, 8.7; S, 13.8%; found: C, 77.5; H, 9.0; S, 13.7%.

2,7-Didecylbenzo[*b*]benzo[4,5]thieno[2,3-*d*]thiophene, C_{10}-BTBT-C_{10}

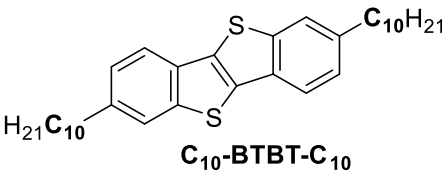

C_{10}-BTBT-C_{10}

Hydrazine hydrate (55%, 3.28 mL, 37.0 mmol) was added to a suspension of **4** (800 mg, 1.46 mmol) and freshly pulverised KOH (800 mg, 14.3 mmol) in 40 mL ethylene glycol and 10 mL ethylene glycol monomethyl ether. The reaction mixture was heated to 200 °C and stirred for 48 h. After the mixture was allowed to cool down to room temperature, it was poured into 100 mL of water and the resulting precipitate was filtered, and subsequently purified by column chromatography over silica using light petroleum as eluent to give **C_{10}-BTBT-C_{10}** (362 mg, 48%) as white crystals; (m.p. 112 °C); ^{1}H NMR (300 MHz, $CDCl_3$): δ 0.87 (6H, t, *J* = 7.0 Hz, CH_3), 1.21−1.43 (28H, m, CH_2), 1.63−1.78 (4H, m, CH_2), 2.75 (4H, t, *J* = 8.0 Hz, CH_2), 7.26 (1H, d, *J* = 1.5 Hz, Ar-H), 7.28 (1H, d, *J* = 1.5 Hz, Ar-H), 7.70 (2H, dd, *J* = 1.5, 0.5 Hz, Ar-H), 7.76 (2H, dd, *J* = 8.0, 0.5 Hz, Ar-H); IR ν_{max}(solid)/cm^{-1}: 2915, 2849, 1460, 1336, 1256, 951, 881, 814, 718, 610; m/z HRMS (ESI-MS): calculated for $C_{34}H_{48}NaS_2$ $[M+Na]^+$: 543.3090; found $[M+Na]^+$: 543.3079; $C_{34}H_{48}S_2$ requires C, 78.4; H, 9.3; S, 12.3%; found: C, 78.3; H, 9.6; S, 12.3%

Photophysical Spectra

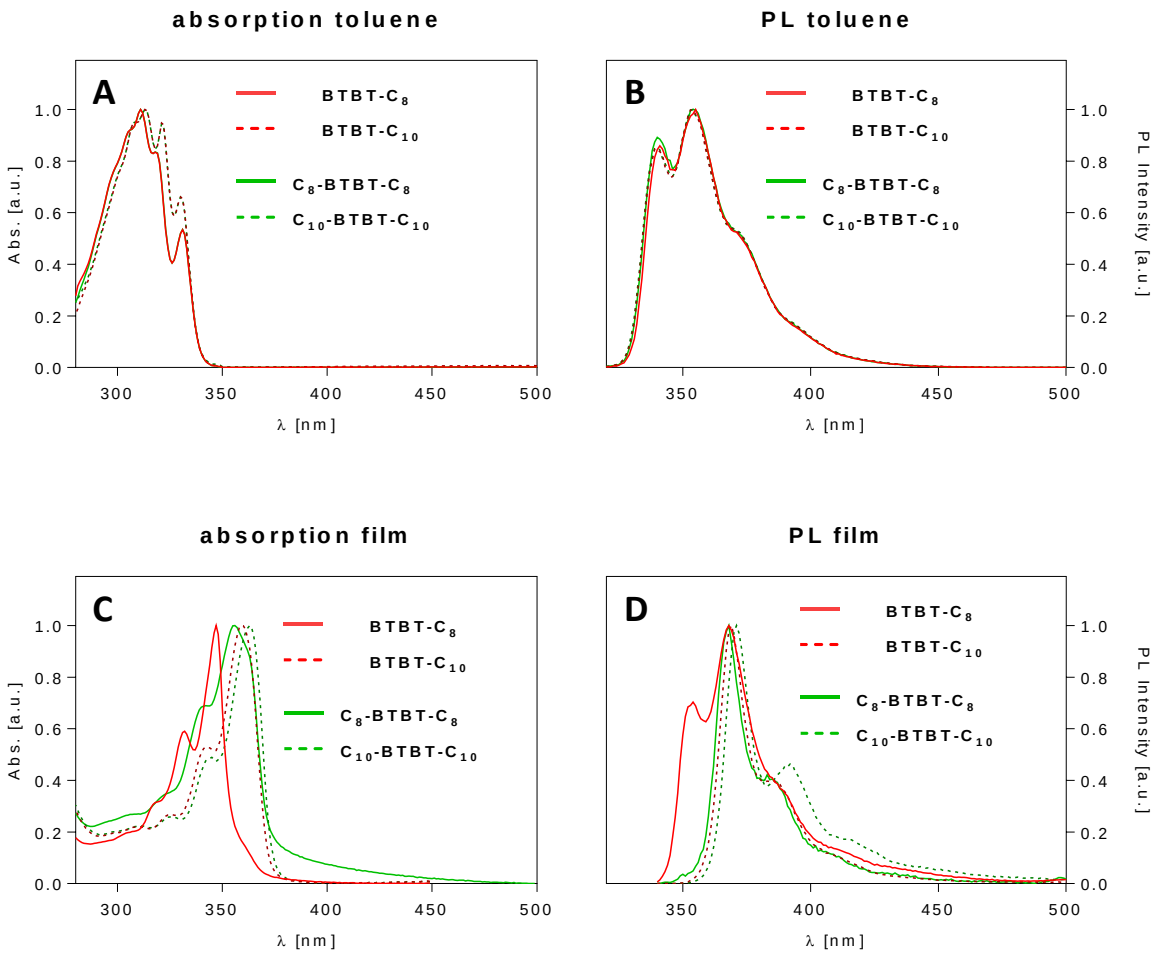

Figure S1. Absorption and photoluminescence (PL) spectra of BTBTs in toluene solution (**A**, **B**) and on evaporated thin films (**C**, **D**).

Single Crystal XRD of BTBT-C_{10}

Single crystal X-ray diffraction data of **BTBT-C_{10}** were obtained at the MX1 beamline at the Australian Synchrotron.{Cowieson, 2015 #28069} Data collection was obtained with a 360° phi scan, wavelength: $\lambda = 0.7108$ Å and with temperature: T = 100(2) K. Data acquisition was performed using Blu-Ice.[39] Data integration was performed using the XDS package software.[40] Using Olex2 graphical interface,[41] the crystal structure was solved with the ShelXT[42] and refined with the ShelXL.[43] The crystallographic information file has been deposited with the CCDC (deposition number 1857063). Despite many attempts, only low quality intrinsically twinned crystals were obtained resulting, in broad diffraction, low resolution data and higher residuals than ideal. Nevertheless, the quality of the diffraction data is more than sufficient to unambiguously determine the connectivity of the structure.

Table S2. Crystal data and structure refinement for **BTBT-C_{10}**.

Empirical formula	$C_{24}H_{28}S_2$
Formula weight	380.58
Temperature/K	100(2)
Crystal system	triclinic
Space group	P-1
a/Å	5.9320(12)
b/Å	7.6920(15)
c/Å	44.704(9)
α/°	86.28(3)
β/°	88.72(3)
γ/°	89.85(3)
Volume/Å^3	2035.0(7)
Z	4
ρ_{calc}g/cm^3	1.242
μ/mm^{-1}	0.267
F(000)	816.0
Crystal size/mm^3	0.15 × 0.07 × 0.01
Radiation	Synchrotron (λ = 0.7108)
2Θ range for data collection/°	5.308 to 54.834
Index ranges	$-7 \le h \le 7$, $-9 \le k \le 9$, $-57 \le l \le 57$
Reflections collected	22513
Independent reflections	7616 [R_{int} = 0.0892, R_{sigma} = 0.0988]
Data/restraints/parameters	7616/312/292
Goodness-of-fit on F^2	1.859
Final R indexes [I>=2σ (I)]	R_1 = 0.1636, wR_2 = 0.4605
Final R indexes [all data]	R_1 = 0.1941, wR_2 = 0.4839
Largest diff. peak/hole / e Å^{-3}	1.17/-1.23

XRD and AFM Measurements

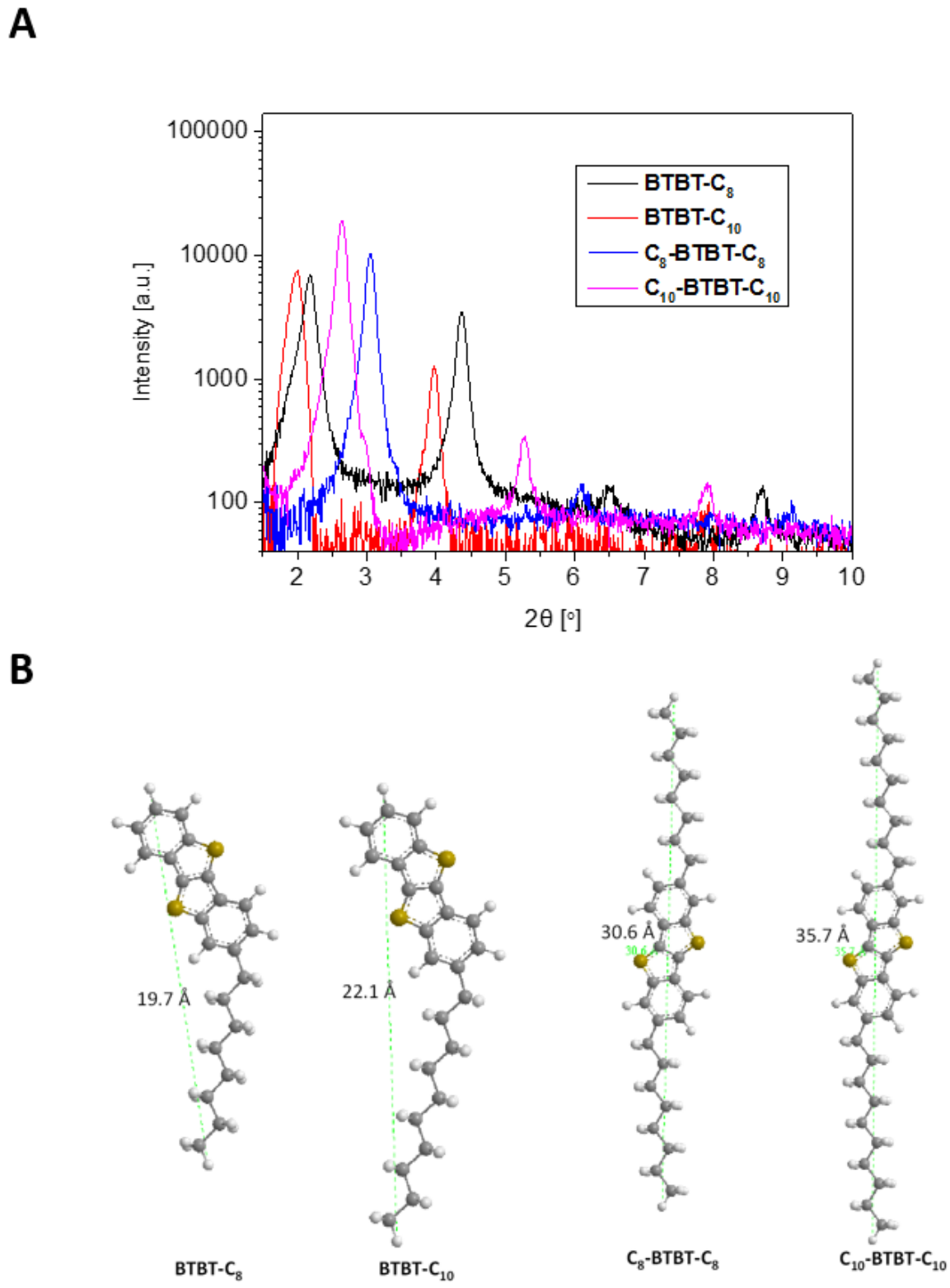

Figure S2. Grazing Angle XRD spectra of the evaporated layers of four BTBT derivatives (A); The calculated layer spacing (**Table S3**) corresponds well with the length of the molecule in the case of di-alkylated BTBTs and mixture of mono- and double-layers for mono-alkylated BTBT derivatives (B).

Table S3. Summary of XRD analysis.

Diffraction order	BTBT-C_8		BTBT-C_{10}		C_8-BTBT-C_8		C_{10}-BTBT-C_{10}	
	2θ [^{O}]	d [Å]	2θ [^{O}]	d [Å]	2θ [^{O}]	d [Å]	2θ [^{O}]	d (Å)
N = 1	2.18	40.49	1.99	44.35	3.04	29.04	2.63	33.56
N = 2	4.37	40.41	3.97	44.47	6.07	29.10	5.27	33.51
N = 3	6.50	40.76	5.91	44.82	9.1	29.13	7.90	33.55
N = 4	8.69	40.67	7.89	44.78	–	–	–	–
Average		40.6±0.1		44.6±0.2		29.09±0.04		33.54±0.02

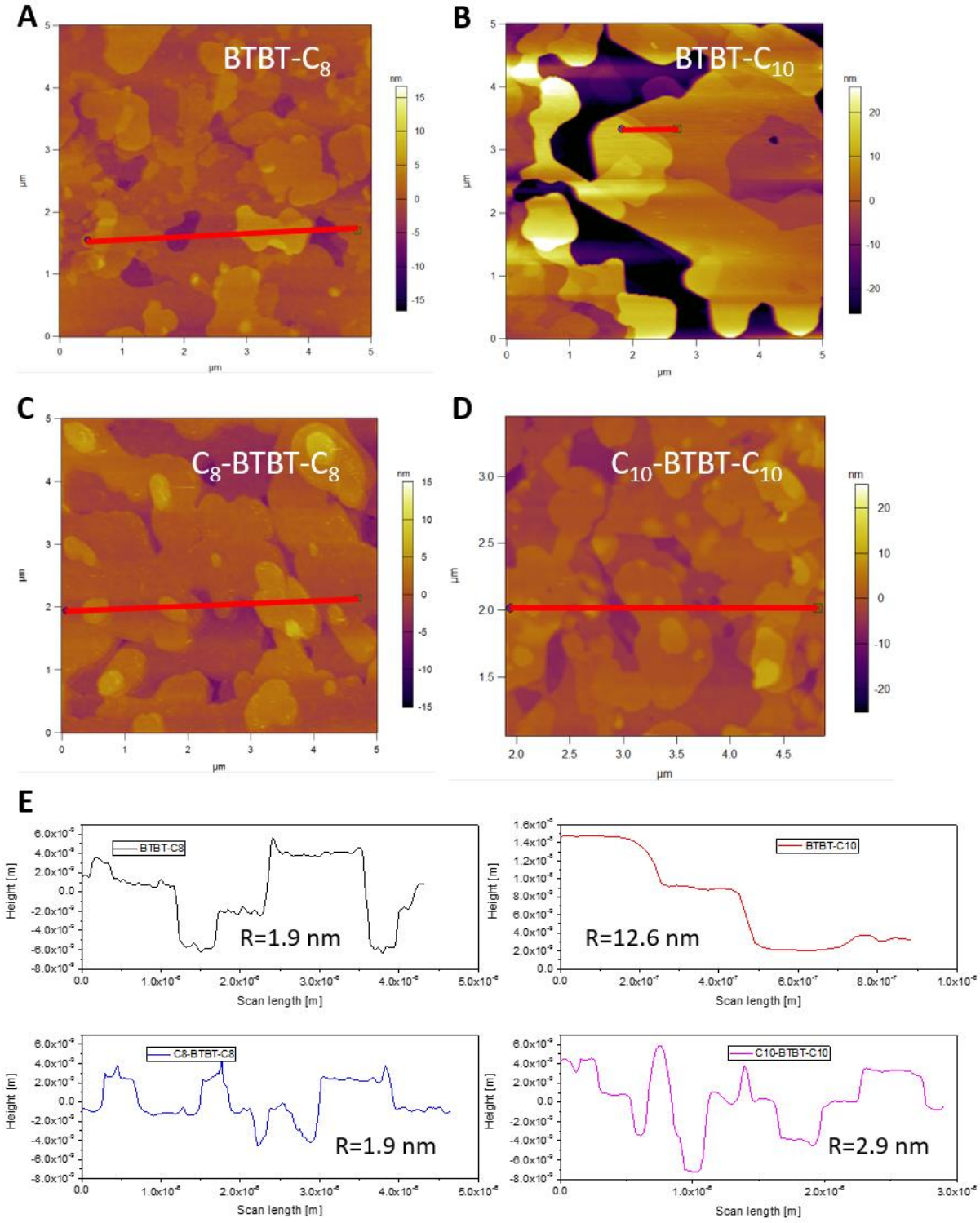

Figure S3. AFM images of the evaporated layers of BTBT derivatives: **BTBT-C$_8$** (A), **BTBT-C$_{10}$** (B), **C$_8$-BTBT-C$_8$** (C), **C$_{10}$-BTBT-C$_{10}$** (D) and the respective profiles of their cross-sections (indicated in red), showing step height and giving the surface roughness (E).

Electrical Measurements

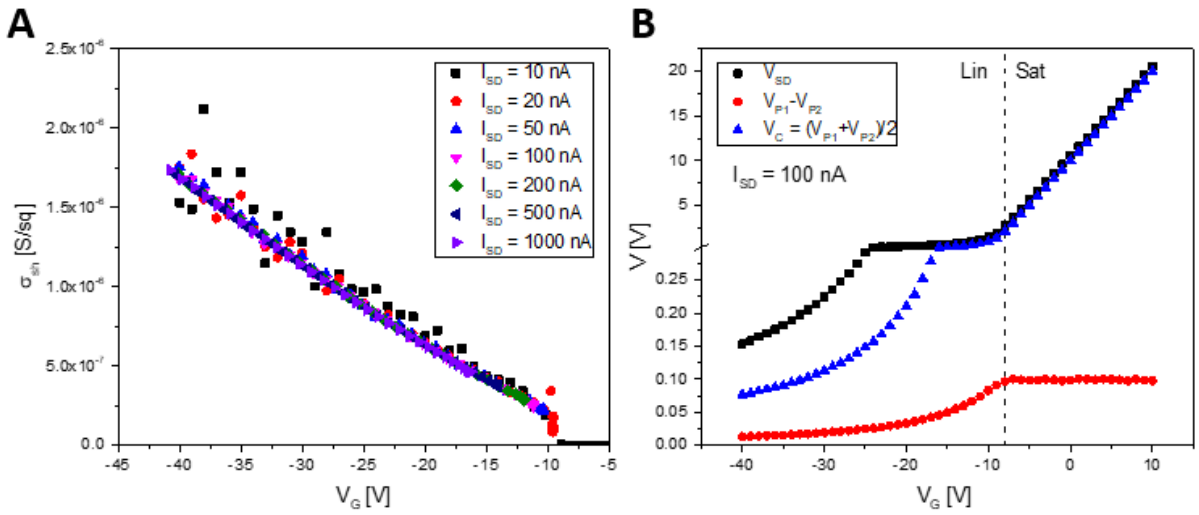

Figure S4. gVDP conductivity obtained **for C$_8$-BTBT-C$_8$** device using currents ranging from 10 nA to 1000 nA (A). Source-drain bias and two derived potentials – V_C and V_{P1}-V_{P2} – showing clear border between linear and saturation regime (B).

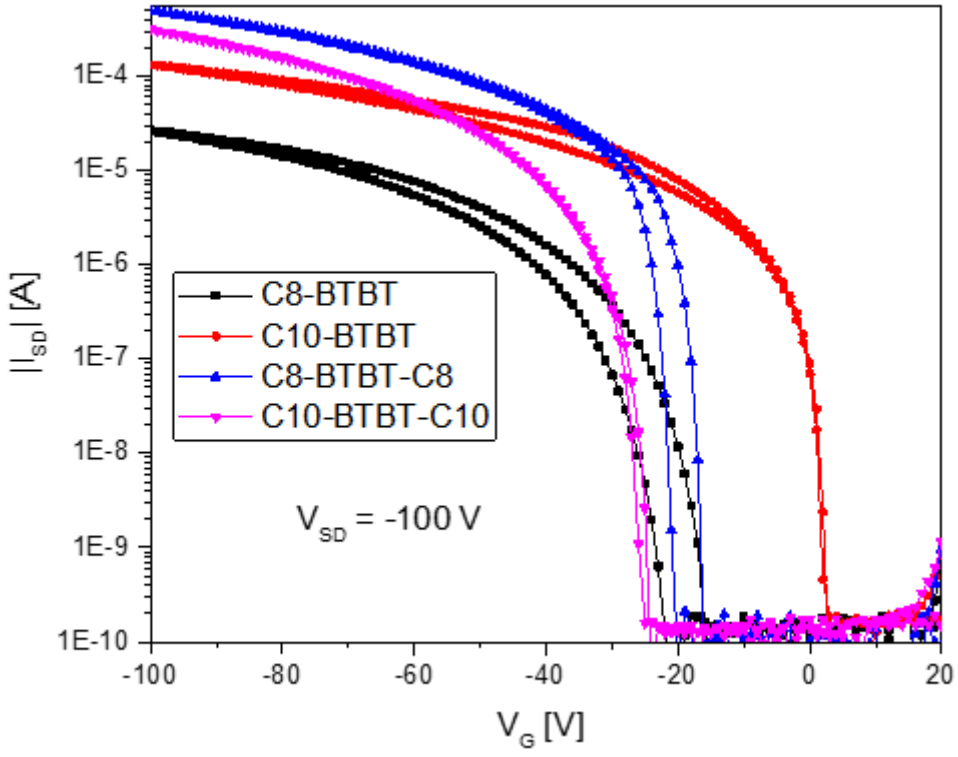

Figure S5. Comparison of transfer characteristics of transistors with the channel length L = 400 μm and channel width W = 1 mm prepared using different BTBT derivatives.

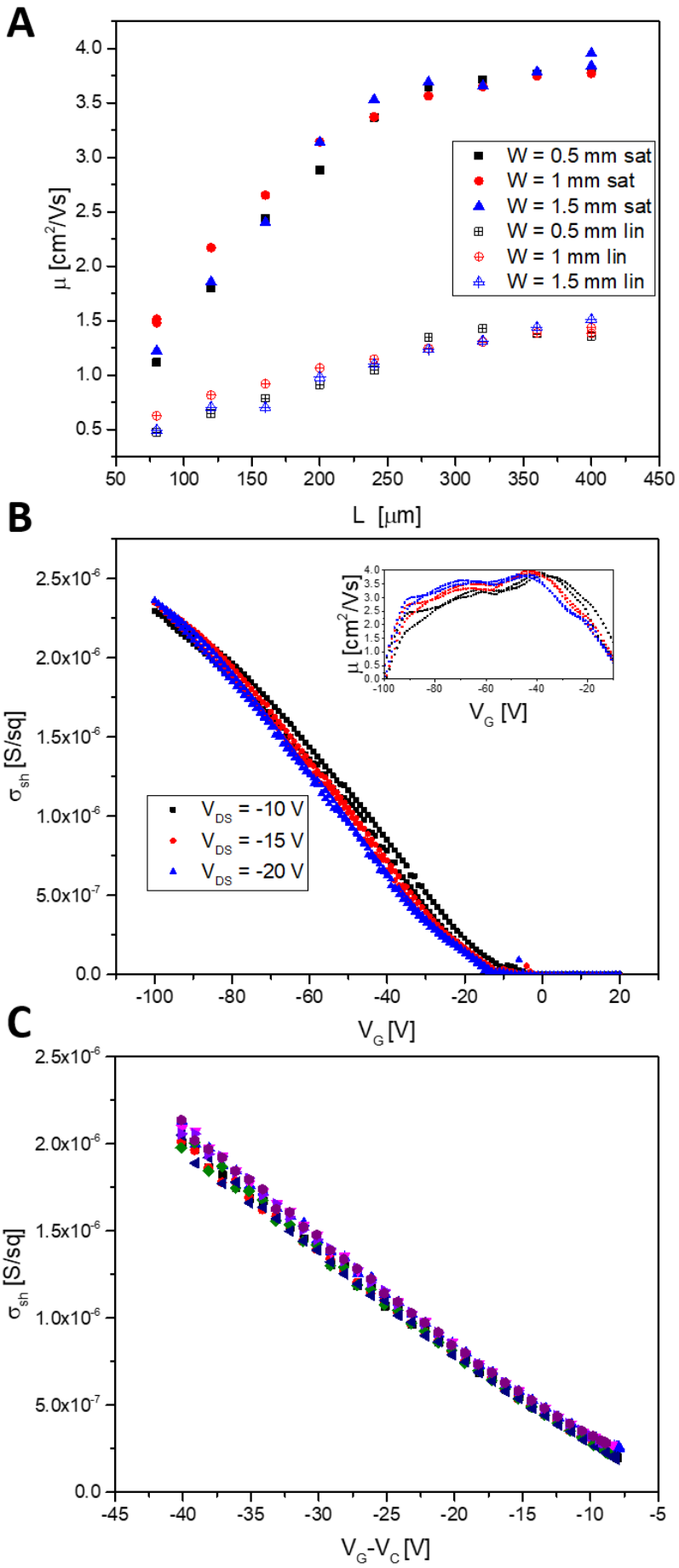
A
μ [cm²/Vs]
L [μm]
W = 0.5 mm sat
W = 1 mm sat
W = 1.5 mm sat
W = 0.5 mm lin
W = 1 mm lin
W = 1.5 mm lin
B
σsh [S/sq]
VG [V]
μ [cm²/Vs]
VG [V]
VDS = -10 V
VDS = -15 V
VDS = -20 V
C
σsh [S/sq]
VG-VC [V]

Figure S6. Mobility characteristics obtained for **C_{10}-BTBT-C_{10}** using three different techniques: linear (lin) and saturation (sat) mobility extracted from Transistor Transmission Line measurements for various channel widths and increasing length (A); conductivity plot for the gated four point probe device for driven at varying source-drain voltages with the extracted mobility in the inset (B); gated van der Pauw conductivity plot combining 8 measurements under different orientations for a single device (C).

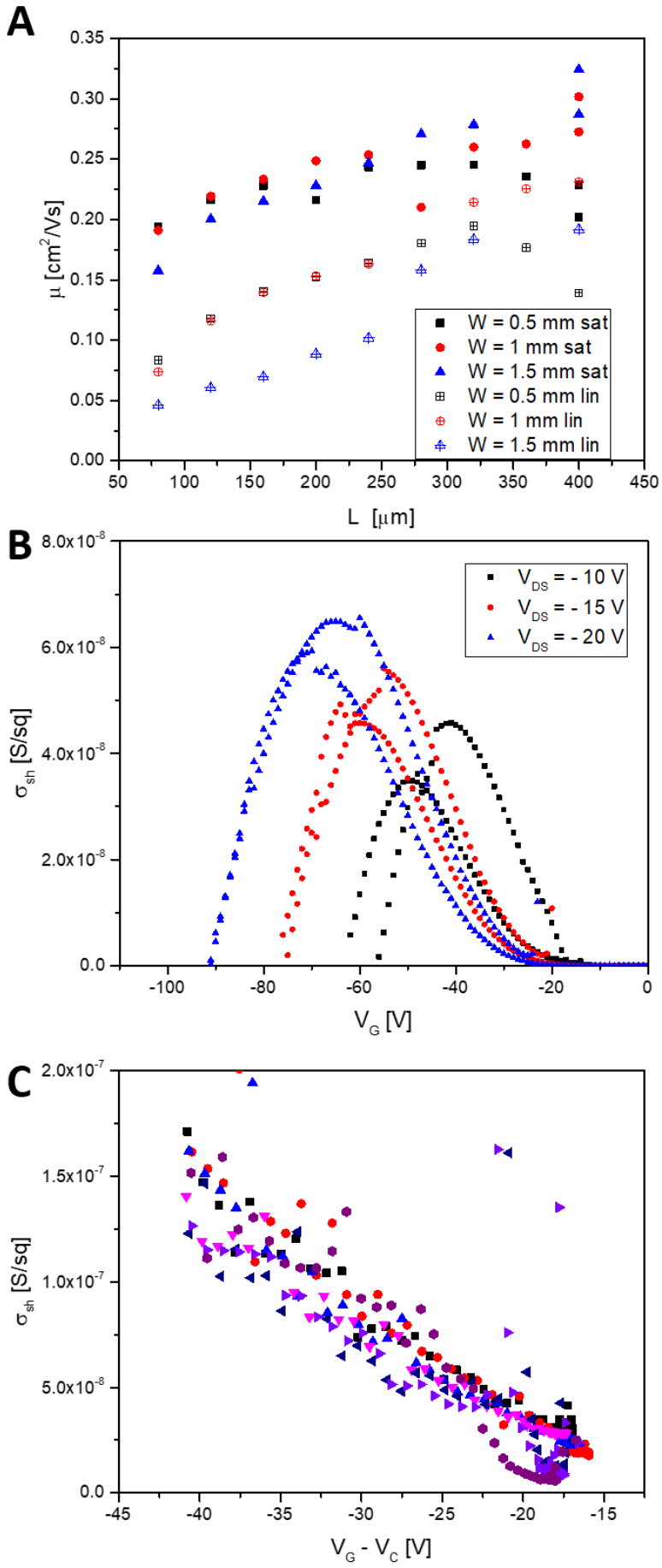
A
0.35
0.30
0.25
0.20
0.15
0.10
0.05
0.00
μ [cm²/Vs]
W = 0.5 mm sat
W = 1 mm sat
W = 1.5 mm sat
W = 0.5 mm lin
W = 1 mm lin
W = 1.5 mm lin
50
100
150
200
250
300
350
400
450
L [μm]
B
8.0x10⁻⁸
6.0x10⁻⁸
4.0x10⁻⁸
2.0x10⁻⁸
0.0
σsh [S/sq]
VDS = - 10 V
VDS = - 15 V
VDS = - 20 V
-100
-80
-60
-40
-20
0
VG [V]
C
2.0x10⁻⁷
1.5x10⁻⁷
1.0x10⁻⁷
5.0x10⁻⁸
0.0
σsh [S/sq]
-45
-40
-35
-30
-25
-20
-15
VG - VC [V]

Figure S7. Mobility characteristics obtained for **BTBT-C$_8$** using three different techniques: linear (lin) and saturation (sat) mobility extracted from Transistor Transmission Line measurements for various channel widths and increasing length (A); conductivity plot for the gated four point probe device for driven at varying source-drain voltages with the extracted mobility in the inset (B); gated van der Pauw conductivity plot combining 8 measurements under different orientations for a single device (C).

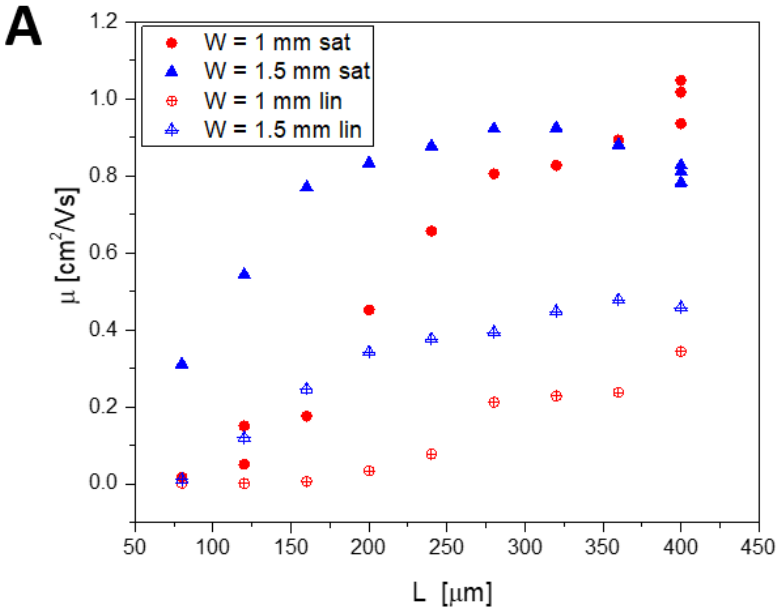
A
W = 1 mm sat
W = 1.5 mm sat
W = 1 mm lin
W = 1.5 mm lin
μ [cm²/Vs]
L [μm]

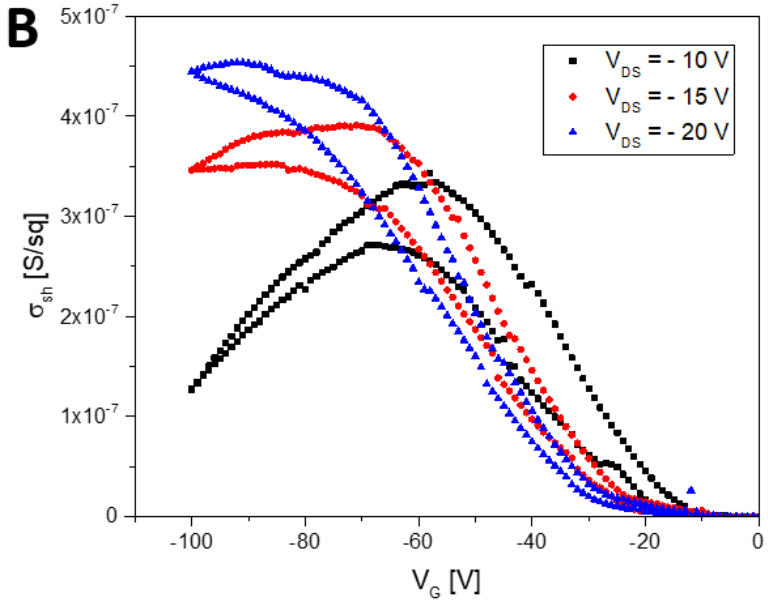
B
V_DS = - 10 V
V_DS = - 15 V
V_DS = - 20 V
σ_sh [S/sq]
V_G [V]

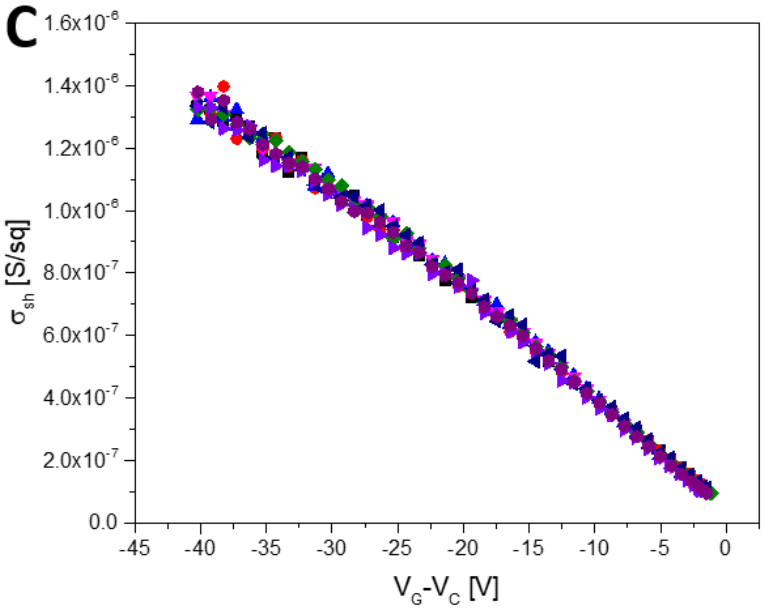
C
σ_sh [S/sq]
V_G-V_C [V]

Figure S8. Mobility characteristics obtained for **BTBT-C$_{10}$** using three different techniques: linear (lin) and saturation (sat) mobility extracted from Transistor Transmission Line measurements for various channel widths and increasing length (A); conductivity plot for the gated four point probe device for driven at varying source-drain voltages with the extracted mobility in the inset (B); gated van der Pauw conductivity plot combining 8 measurements under different orientations for a single device (C).

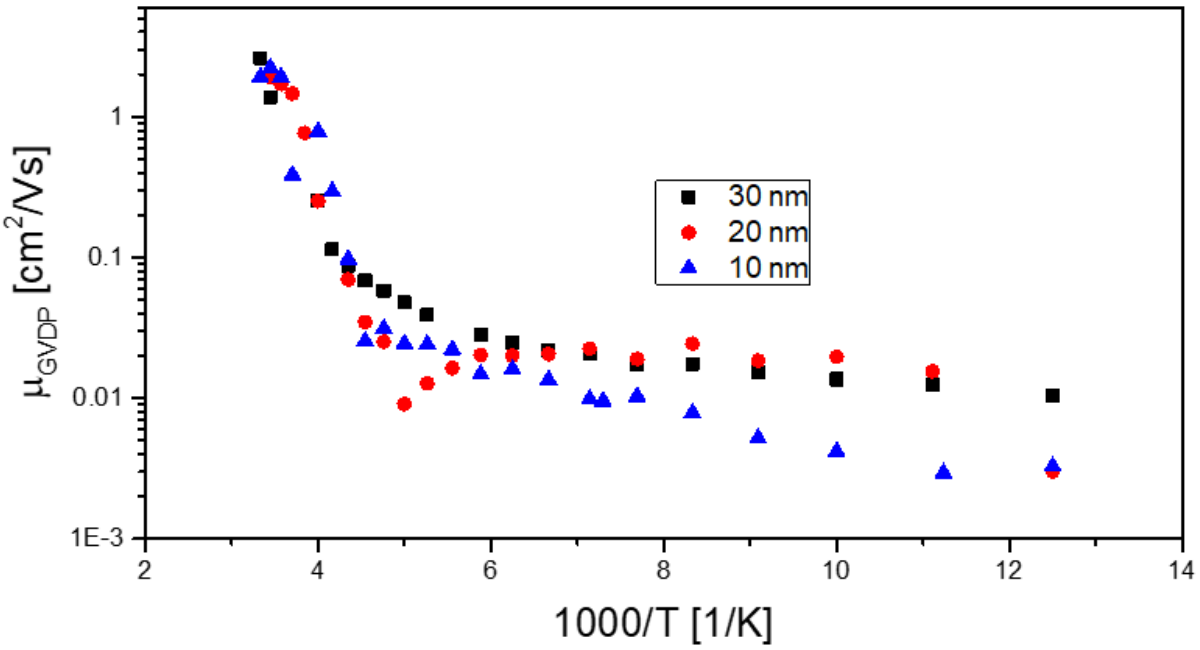

Figure S9. Mobility plotted as a function of inverse temperature for **C$_8$-BTBT-C$_8$** devices with thickness of 10, 20 and 30 nm.

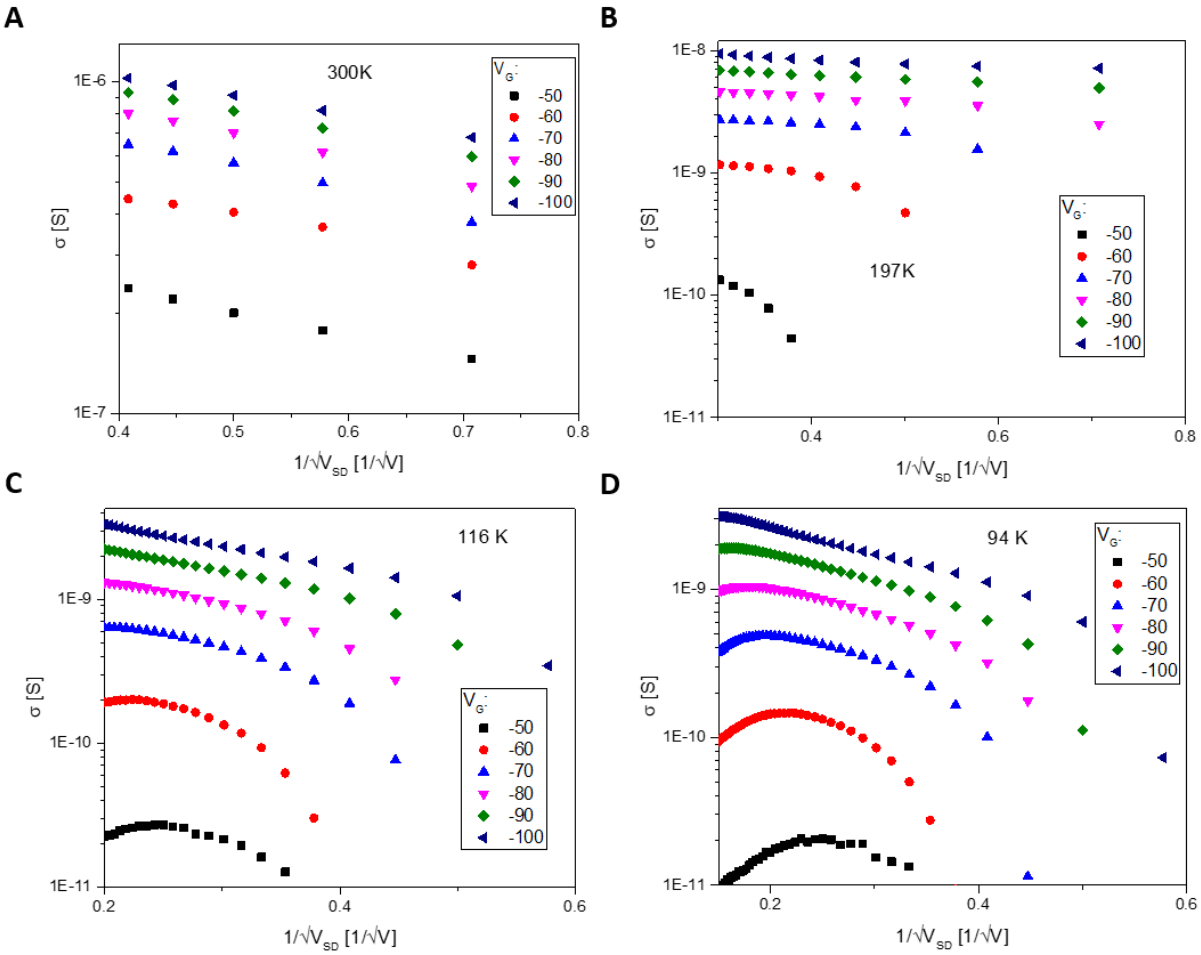

Figure S10. Channel conductivity of **C_8-BTBT-C_8** devices plotted vs $1/\sqrt{V_{SD}}$ (proportional to the $1/\sqrt{E}$) for different gate voltages and temperatures over T_C (A), just below T_C (B) and further below T_C (C and D).

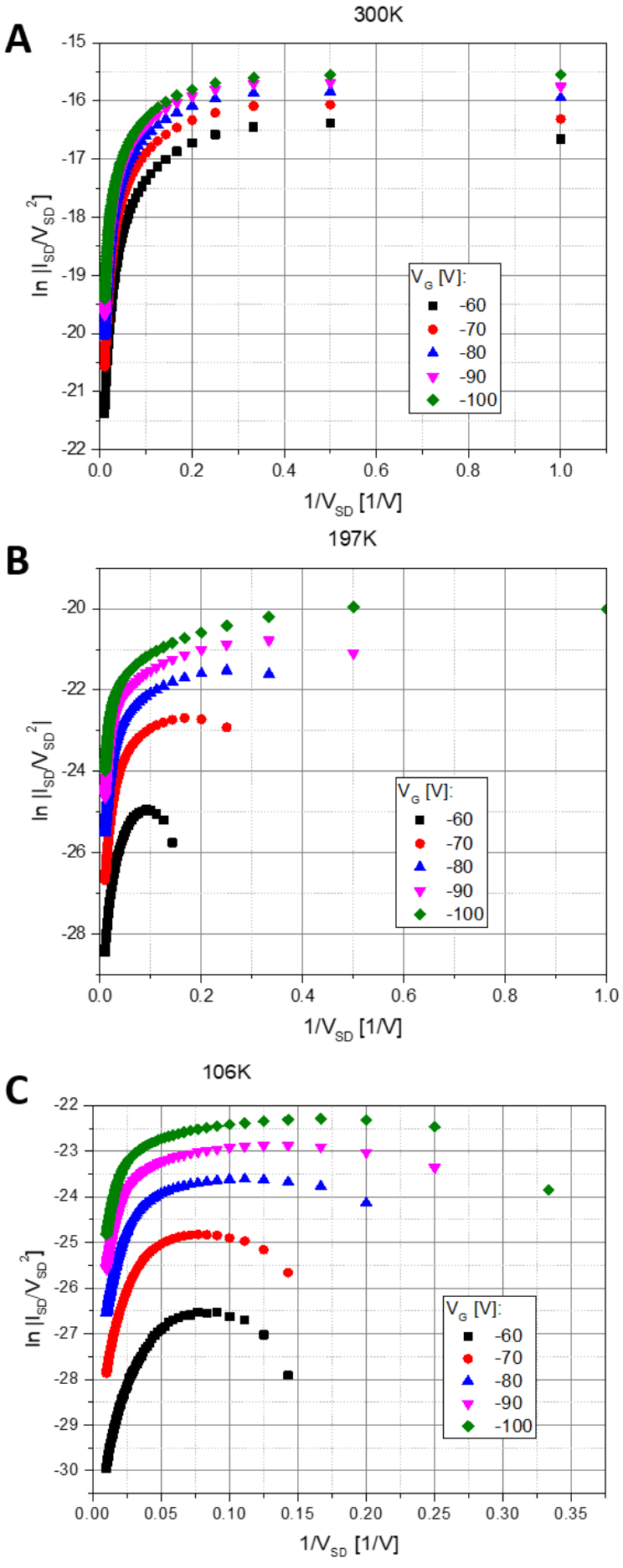
A
300K
ln |I_SD/V_SD^2|
1/V_SD [1/V]
V_G [V]:
-60
-70
-80
-90
-100
B
197K
ln |I_SD/V_SD^2|
1/V_SD [1/V]
V_G [V]:
-60
-70
-80
-90
-100
C
106K
ln |I_SD/V_SD^2|
1/V_SD [1/V]
V_G [V]:
-60
-70
-80
-90
-100

Figure S11. Fowler-Nordheim plots for 20 nm thick **C_8-BTBT-C_8** device for different gate voltages and temperatures: 300 K (A), 197 K (B) and 106 K (C). Logarithmic shape of curves indicates rectangular shape of the energy barrier in all the cases.

References

(1) Takimiya, K.; Osaka, I.; Mori, T.; Nakano, M. Organic Semiconductors Based on [1]Benzothieno[3,2-b][1]Benzothiophene Substructure. *Acc. Chem. Res.* **2014**, *47*, 1493–1502.

(2) Ullah, M.; Wawrzinek, R.; Maasoumi, F.; Lo, S.-C.; Namdas, E. B. Semitransparent and Low-Voltage Operating Organic Light-Emitting Field-Effect Transistors Processed at Low Temperatures. *Adv. Opt. Mater.* **2016**, *4*, 1022–1026.

(3) Soeda, J.; Hirose, Y.; Yamagishi, M.; Nakao, A.; Uemura, T.; Nakayama, K.; Uno, M.; Nakazawa, Y.; Takimiya, K.; Takeya, J. Solution-Crystallized Organic Field-Effect Transistors with Charge-Acceptor Layers: High-Mobility and Low-Threshold-Voltage Operation in Air. *Adv. Mater.* **2011**, *23*, 3309–3314.

(4) Li, Y.; Liu, C.; Kumatani, A.; Darmawan, P.; Minari, T.; Tsukagoshi, K. Surface Selectively Deposited Organic Single-Crystal Transistor Arrays with High Device Performance. *Mol. Cryst. Liq. Cryst.* **2012**, *566*, 13–17.

(5) Fujieda, I.; Iizuka, N.; Onishi, Y. Directional Solidification of C8-BTBT Films Induced by Temperature Gradients and Its Application for Transistors. *Proc. SPIE* **2015**, *9360*, 936012.

(6) Ruzié, C.; Karpinska, J.; Laurent, A.; Sanguinet, L.; Hunter, S.; Anthopoulos, T. D.; Lemaur, V.; Cornil, J.; Kennedy, A. R.; Fenwick, O.; *et al*. Design, Synthesis, Chemical Stability, Packing, Cyclic Voltammetry, Ionisation Potential, and Charge Transport of [1]Benzothieno[3,2-b][1]Benzothiophene Derivatives. *J. Mater. Chem. C* **2016**, *4*, 4863–4879.

(7) Minemawari, H.; Yamada, T.; Matsui, H.; Tsutsumi, J.; Haas, S.; Chiba, R.; Kumai, R.; Hasegawa, T. Inkjet Printing of Single-Crystal Films. *Nature* **2011**, *475*, 364–367.

(8) He, D.; Zhang, Y.; Wu, Q.; Xu, R.; Nan, H.; Liu, J.; Yao, J.; Wang, Z.; Yuan, S.; Li, Y.; *et al*. Two-Dimensional Quasi-Freestanding Molecular Crystals for High-Performance Organic Field-Effect Transistors. *Nat. Commun.* **2014**, *5*, 5162.

(9) Wang, Q.; Qian, J.; Li, Y.; Zhang, Y.; He, D.; Jiang, S.; Wang, Y.; Wang, X.; Pan, L.; Wang, J.; *et al*. 2D Single-Crystalline Molecular Semiconductors with Precise Layer Definition Achieved by Floating-Coffee-Ring-Driven Assembly. *Adv. Funct. Mater.* **2016**, *26*, 3191–3198.

(10) Ebata, H.; Izawa, T.; Miyazaki, E.; Takimiya, K.; Ikeda, M.; Kuwabara, H.; Yui, T. Highly Soluble [1]Benzothieno[3,2-b]Benzothiophene (BTBT) Derivatives for High-Performance, Solution-Processed Organic Field-Effect Transistors. *J. Am. Chem. Soc.* **2007**, *129*, 15732–15733.

(11) Yuan, Y.; Giri, G.; Ayzner, A. L.; Zoombelt, A. P.; Mannsfeld, S. C. B.; Chen, J.; Nordlund, D.; Toney, M. F.; Huang, J.; Bao, Z. Ultra-High Mobility Transparent Organic Thin Film Transistors Grown by an off-Centre Spin-Coating Method. *Nat. Commun.* **2014**, *5*, 3005.

(12) Izawa, T.; Miyazaki, E.; Takimiya, K. Molecular Ordering of High-Performance Soluble Molecular Semiconductors and Re-Evaluation of Their Field-Effect Transistor Characteristics. *Adv. Mater.* **2008**, *20*, 3388–3392.

(13) Liu, C.; Minari, T.; Lu, X.; Kumatani, A.; Takimiya, K.; Tsukagoshi, K. Solution-Processable Organic Single Crystals with Bandlike Transport in Field-Effect Transistors. *Adv. Mater.* **2011**, *23*, 523–526.

(14) Minari, T.; Kano, M.; Miyadera, T.; Wang, S.-D.; Aoyagi, Y.; Tsukagoshi, K. Surface Selective Deposition of Molecular Semiconductors for Solution-Based Integration of Organic Field-Effect Transistors. *Appl. Phys. Lett.* **2009**, *94*, 093307.

(15) Huang, Y.; Sun, J.; Zhang, J.; Wang, S.; Huang, H.; Zhang, J.; Yan, D.; Gao, Y.; Yang,

J. Controllable Thin-Film Morphology and Structure for 2,7-Dioctyl[1]Benzothieno[3,2-b][1]Benzothiophene (C8BTBT) Based Organic Field-Effect Transistors. *Org. Electron.* **2016**, *36*, 73–81.

(16) He, D.; Qiao, J.; Zhang, L.; Wang, J.; Lan, T.; Qian, J.; Li, Y.; Shi, Y.; Chai, Y.; Lan, W.; *et al*. Ultrahigh Mobility and Efficient Charge Injection in Monolayer Organic Thin-Film Transistors on Boron Nitride. *Sci. Adv.* **2017**, *3*, e1701186.

(17) Generali, G.; Soldano, C.; Facchetti, A.; Muccini, M. P-176: Innovative Trilayer Organic Light Emitting Transistor (OLET) Structure for Blue Emission. *SID Symp. Dig. Tech. Pap.* **2016**, *47*, 1779–1782.

(18) Choi, J.; Joo, M.; Seong, H.; Park, H.; Park, C. W.; Im, S. G. Phase Synthesized High-k , Ultrathin Polymer Gate Dielectrics Flexible, Low-Power Thin-Film Transistors (TFTs) Made of Vapor- Phase Synthesized High-k , Ultrathin Polymer Gate Dielectrics. *ACS App. Mater. Interfaces* **2017**, *9*, 20808–20817.

(19) Rolin, C.; Kang, E.; Lee, J.-H.; Borghs, G.; Heremans, P.; Genoe, J. Charge Carrier Mobility in Thin Films of Organic Semiconductors by the Gated van Der Pauw Method. *Nat. Commun.* **2017**, *8*, 14975.

(20) Choe, Y.-S.; Yi, M. H.; Kim, J.-H.; Ryu, G.-S.; Noh, Y.-Y.; Kim, Y. H.; Jang, K.-S. Crosslinked Polymer-Mixture Gate Insulator for High-Performance Organic Thin-Film Transistors. *Org. Electron.* **2016**, *36*, 171–176.

(21) Temiño, I.; Del Pozo, F. G.; Ajayakumar, M. R.; Galindo, S.; Puigdollers, J.; Mas-Torrent, M. A Rapid, Low-Cost, and Scalable Technique for Printing State-of-the-Art Organic Field-Effect Transistors. *Adv. Mater. Technol.* **2016**, 1600090.

(22) Wu, K.; Li, H.; Li, L.; Zhang, S.; Chen, X.; Xu, Z.; Zhang, X.; Hu, W.; Chi, L.; Gao, X.; *et al*. Controlled Growth of Ultrathin Film of Organic Semiconductors by Balancing the Competitive Processes in Dip-Coating for Organic Transistors. *Langmuir* **2016**, *32*, 6246–6254.

(23) Yoon, J.-Y.; Jeong, S.; Lee, S. S.; Kim, Y. H.; Ka, J.-W.; Yi, M. H.; Jang, K.-S. Enhanced Performance of Solution-Processed Organic Thin-Film Transistors with a Low-Temperature-Annealed Alumina Interlayer between the Polyimide Gate Insulator and the Semiconductor. *ACS Appl. Mater. Interfaces* **2013**, *5*, 5149–5155.

(24) Cho, J.; Higashino, T.; Mori, T. Band-like Transport down to 20 K in Organic Single-Crystal Transistors Based on Dioctylbenzothienobenzothiophene. *Appl. Phys. Lett.* **2015**, *106*, 193303.

(25) Ren, H.; Cui, N.; Tang, Q.; Tong, Y.; Zhao, X.; Liu, Y. High-Performance, Ultrathin, Ultraflexible Organic Thin-Film Transistor Array via Solution Process. *Small* **2018**, 1801020.

(26) Haase, K.; Teixeira, C.; Hauenstein, C.; Zheng, Y.; Hambsch, M.; Mannsfeld, S. C. B. High-Mobility , Solution-Processed Organic Field-Effect Transistors from C8-BTBT : Polystyrene Blends. *Adv. Electron. Mater.* **2018**, *1800076*.

(27) Jang, K.-S.; Kim, W. S.; Won, J.-M.; Kim, Y.-H.; Myung, S.; Ka, J.-W.; Kim, J.; Ahn, T.; Yi, M. H. Surface Modification of Polyimide Gate Insulators for Solution-Processed 2,7-Didecyl[1]Benzothieno[3,2-b][1]Benzothiophene (C10-BTBT) Thin-Film Transistors. *Phys. Chem. Chem. Phys.* **2013**, *15*, 950–956.

(28) Tsutsui, Y.; Schweicher, G.; Chattopadhyay, B.; Sakurai, T.; Arlin, J.-B.; Ruzié, C.; Aliev, A.; Ciesielski, A.; Colella, S.; Kennedy, A. R.; *et al*. Unraveling Unprecedented Charge Carrier Mobility through Structure Property Relationship of Four Isomers of Didodecyl[1]Benzothieno[3,2-b][1]Benzothiophene. *Adv. Mater.* **2016**, *28*, 7106–7114.

(29) Amin, A. Y.; Khassanov, A.; Reuter, K.; Meyer-friedrichsen, T.; Halik, M. Low-Voltage Organic Field Effect Transistors with a 2-Tridecyl[1]Benzothieno[3,2-b][1]Benzothiophene Semiconductor Layer. *J. Am. Chem. Soc.* **2012**, *134*, 16548–16550.

(30) Dietrich, H.; Scheiner, S.; Portilla, L.; Zahn, D.; Halik, M. Improving the Performance of Organic Thin-Film Transistors by Ion Doping of Ethylene-Glycol-Based Self-Assembled Monolayer Hybrid Dielectrics. *Adv. Mater.* **2015**, *27*, 8023–8027.
(31) Kunii, M.; Iino, H.; Hanna, J. Organic Field-Effect Transistor Fabricated Using Highly Ordered Liquid Crystal With Low-k Gate Dielectric. *IEEE Electr. Dev. Lett.* **2016**, *37*, 486–488.
(32) Iino, H.; Usui, T.; Hanna, J.-I. Liquid Crystals for Organic Thin-Film Transistors. *Nat. Commun.* **2015**, *6*, 6828.
(33) Hamai, T.; Arai, S.; Hasegawa, T. Effects of Tunneling-Based Access Resistance in Layered Single-Crystalline Organic Transistors. *J. Mater. Res.* **2018**, 1–14.
(34) He, Y.; Sezen, M.; Zhang, D.; Li, A.; Yan, L.; Yu, H.; He, C.; Goto, O.; Loo, Y.-L.; Meng, H. High Performance OTFTs Fabricated Using a Calamitic Liquid Crystalline Material of 2-(4-Dodecyl Phenyl)[1]Benzothieno[3,2-b][1]Benzothiophene. *Adv. Electron. Mater.* **2016**, *2*, 1600179.
(35) Saito, M.; Osaka, I.; Miyazaki, E.; Takimiya, K.; Kuwabara, H.; Ikeda, M. One-Step Synthesis of [1]Benzothieno[3,2-b][1]Benzothiophene from o-Chlorobenzaldehyde. *Tetrahedron Lett.* **2011**, *52*, 285–288.
(36) Combe, C. M. S.; Biniek, L.; Schroeder, B. C.; McCulloch, I. Synthesis of [1]Benzothieno[3,2-b][1]Benzothiophene Pendant and Norbornene Random Co-Polymers via Ring Opening Metathesis. *J. Mater. Chem. C* **2014**, *2*, 538–541.
(37) Niebel, C.; Kim, Y.; Ruzie, C.; Karpinska, J.; Chattopadhyay, B.; Schweicher, G.; Richard, A.; Lemaur, V.; Olivier, Y.; Cornil, J.; *et al*. Thienoacene Dimers Based on the Thieno[3,2-b]Thiophene Moiety: Synthesis, Characterization and Electronic Properties. *J. Mater. Chem. C* **2015**, *3*, 674–685.
(38) Inoue, S.; Minemawari, H.; Tsutsumi, J.; Chikamatsu, M.; Yamada, T.; Horiuchi, S.; Tanaka, M.; Kumai, R.; Yoneya, M.; Hasegawa, T. Effects of Substituted Alkyl Chain Length on Solution-Processable Layered Organic Semiconductor Crystals. *Chem. Mater.* **2015**, *27*, 3809–3812.
(39) McPhillips, T. M.; McPhillips, S. E.; Chiu, H. J.; Cohen, A. E.; Deacon, A. M.; Ellis, P. J.; Garman, E.; Gonzalez, A.; Sauter, N. K.; Phizackerley, R. P.; *et al*. Blu-Ice and the Distributed Control System: Software for Data Acquisition and Instrument Control at Macromolecular Crystallography Beamlines. *J. Synchrotron Radiat.* **2002**, *9*, 401–406.
(40) Kabsch, W. Xds. *Acta Crystallogr. Sect. D* **2010**, *66*, 125–132.
(41) Dolomanov, O. V.; Bourhis, L. J.; Gildea, R. J.; Howard, J. A. K.; Puschmann, H. OLEX2: A Complete Structure Solution, Refinement and Analysis Program. *J. Appl. Crystallogr.* **2009**, *42*, 339–341.
(42) Sheldrick, G. M. SHELXT-Integrated Space-Group and Crystal-Structure Determination. *Acta Crystallogr. Sect. A* **2015**, *71*, 3–8.
(43) Sheldrick, G. M. Crystal Structure Refinement with SHELXL. *Acta Crystallogr. Sect. C* **2015**, *71*, 3–8.